



On-Site Measurement on Compaction Characteristics of Coal Gangue and Surface Subsidence Disaster in Deep Backfilling Mining

Jiaqi Wang^{1,2}, Qiang Zhang^{1,2*}, Wei Yin³, Shengming Qi^{1,2}, Difa Gao^{1,2} and Dan Ma^{1,2*}

¹School of Mines, China University of Mining and Technology, Xuzhou, China, ²State Key Laboratory of Coal Resources and Safe Mining, China University of Mining and Technology, Xuzhou, China, ³The Key Laboratory for Traffic and Transportation Security of Jiangsu Province, Huaiyin Institute of Technology, Huaian, China

OPEN ACCESS

Edited by:

Jie Chen,
Chongqing University, China

Reviewed by:

Qinglei Yu,
Northeastern University, China
Yang Ke,
Anhui University of Science and
Technology, China

*Correspondence:

Qiang Zhang
leafkky@163.com
Dan Ma
dan.ma@cumt.edu.cn

Specialty section:

This article was submitted to
Geohazards and Georisks,
a section of the journal
Frontiers in Earth Science

Received: 13 June 2021

Accepted: 29 September 2021

Published: 20 October 2021

Citation:

Wang J, Zhang Q, Yin W, Qi S, Gao D
and Ma D (2021) On-Site
Measurement on Compaction
Characteristics of Coal Gangue and
Surface Subsidence Disaster in Deep
Backfilling Mining.
Front. Earth Sci. 9:724476.
doi: 10.3389/feart.2021.724476

Gangue is the main backfilling material in solid backfilling mining, and its compaction characteristics determine the overburden control effect and surface subsidence. Under the action of compaction force and overburden pressure, the gangue will be broken, rotated and occluded, resulting in different compaction characteristics of gangue in the field and laboratory. To this end, a laboratory gangue compaction test system was established to test the compaction characteristics of gangue in the laboratory, such as stress-strain, stress bulk density and stress deformation modulus. Based on actual geological conditions of backfilling mining in the Tangshan coal mine, the characteristics of stress deformation modulus of gangue under different inclination angles and mining heights were tested on-site. Through the Beidou satellite CORS system, the surface subsidence of working face F5001 was monitored. The research results show that the stress deformation modulus of gangue measured in the field is slightly less than that measured in the laboratory, and it is maintained at about 27 MPa under the overburden pressure in the on-site measurement. Backfilling technology with an initial compaction force of 2.5MPa can be used to effectively control the surface subsidence, and the maximum subsidence value is only 61 mm.

Keywords: backfilling mining, compaction characteristics of gangue, deformation modulus, compaction force, surface subsidence

INTRODUCTION

As the main energy source in China, coal still plays an irreplaceable role in economic and social development in the short term. However, the ecological environment damage caused by coal mining and ground collapse cannot be ignored (Xie et al., 2012; Xie et al., 2015a; Xie et al., 2015b). The Chinese government attaches great importance to the problems caused by coal mining subsidence and has issued a series of documents on the treatment of subsidence areas caused by coal mining. The control of strata movement and surface collapse in backfilling mining and the implementation of backfilling mining technology in combination with field work is key work of researchers (Zhang and Wang, 2007; Fall et al., 2008; Shukla et al., 2009).

Solid backfilling mining is a relatively mature backfilling technology and has been widely used in mining areas in Northeast, North and West China. Up to now, solid backfilling mining technology

has gone through three stages: gangue dumping backfilling, mechanized solid non-dense backfilling and mechanized solid full-section dense backfilling. In the solid backfilling mining, gangue is used as backfilling material to fill goaf and support overburden (Ma et al., 2021b). In recent years, research on the mechanical properties of solid backfilling materials and the mechanism of controlling strata movement have been widely performed. Through macroscopic mechanical tests, Malusis et al. (Malusis et al., 2009) studied the compression properties of continuously graded gangue, discontinuously graded gangue and single-grain graded gangue under the three-dimensional loading. Based on the compression test of broken gangue, Li et al. (2018) reconstructed the gangue particles through 3D scanning and established the meso numerical model of gangue particle flow. Besides, the effects of particle gradation and loading rate on the compaction characteristics and lateral pressure coefficient of gangue were mainly studied. Fall et al. (2010) carried out the confined compression experiment of gangue, and analyzed the deformation and crushing characteristics of gangue particles at different immersion heights. Chong et al. (2020) tested the compaction characteristics of gangue granular backfilling materials with different particle sizes, and explored the influence of initial particle size of backfilling materials on the control effect of strata. Zhang et al. (2015) investigated the mesostructure, stress-strain relationship, energy dissipation and roof control effect of five common solid backfilling materials (Ma et al., 2021a).

It can be seen that the mechanical properties of gangue, especially the compaction characteristics, are the focus of backfill mining. The compaction characteristics of gangue affect the overburden control effect and surface collapse (Niu et al., 2014; Meng et al., 2016; Wei et al., 2021). In the above studies, all the mechanical properties of gangue were tested in the laboratory. However, the mechanical properties of gangue are dynamic in the stope, and the pressure situation of gangue in the goaf is more complex than that in the laboratory. In the advance of the working face, the gangue filling body will be rotated, slipped, occluded and broken under loads (Ercikdi et al., 2009; Cao et al., 2018; Zhu et al., 2020). Therefore, it is of great significance to study the actual compaction characteristics of gangue in stope.

Based on the geological conditions and gangue in Tangshan Coal Mine in Hebei Province, China, the confined compression test of gangue was carried out by the self-designed bearing-compression device; the compaction characteristics such as bulk density and deformation modulus of the backfilling body were obtained. Subsequently, the optimal axial pressure was obtained from the test, and applied to the working face F5001. The on-site compaction characteristics monitoring scheme was designed to explore the compaction characteristics under different inclination angles and different mining heights in the process of advancing. Through the developed Beidou satellite CORS monitoring system, the surface subsidence was monitored in this study. This study promotes the development of backfilling mining technology in China.

PROJECT OVERVIEW AND BACKFILLING TECHNOLOGY

Project Overview

Tangshan coal mine is located in Lunan District, Tangshan City, Hebei Province, with a minefield of 37.28 km² and a mining area of 55 km². With convenient transportation, it is the sole state-owned super-large coal mine located in the central area of the city in China. Tangshan Mine adopts the progressive development mode of vertically inclined shaft mining in stages. At present, it has seven vertical shafts and 10 mining production areas, and no major fault. The main coal seams are coal seams 5, 8, 9, and 12, with an average thickness of 2.4, 3.7, 3.5, and 6.4 m, respectively.

Recently, the mining area F has been mined in the Tangshan mine; the working face F5001 was the first mining face, and the mining time was from 2016.10.5–2019.9.16. The average thickness of coal seams was 2.2 m, and the average inclination angle of coal seams was 11°, and the buried depth was about 600 m. The main roof was gray fine sandstone with a thickness of 17.5 m; The immediate roof was grey strip medium and fine sandstone, with a thickness of 3.7–6.0 m. The immediate floor was dark gray mudstone with a thickness of 0.4–1.4 m, and the main floor was gray strip fine sandstone with a thickness of 5.2 m. The strike length of the working face was 639.5 m and the inclined length was 66 m. **Figure 1** shows the location of the Tangshan Mine and the layout of the working face F5001.

Backfilling Method and Technology

Backfilling Mining Method in Tangshan Mine

The full cross-section solid mechanized backfilling mining was adopted in the Tangshan Mine (Livaoglu et al., 2011; Mitchell et al., 2011; Dai et al., 2018). The backfilling system included the ground conveying system, vertical feeding system, underground separation system, underground conveying system and backfilling system (Hawkes and Fellers, 1969; Wijewickreme and Vaid, 1993; Yuan and Sun, 2012). The ground conveying system was mainly used to crush and transport gangue backfilling materials on the ground. The vertical feeding system was used to transport the backfilling materials from the ground to the underground (Li and Sheng, 1995; Louréno et al., 1997; Benzaazoua et al., 1999). The underground separation system was used to separate the gangue contained in the underground coal flow. The underground conveying system was used to transport the gangue from various sources to the backfill working face. The function of the backfilling system was used to fill gangue into goaf. **Figure 2** shows the backfilling system of the Tangshan mine (Zhang et al., 2015).

Backfilling Technology in the Working Face F5001

In the process of mining, the inclination angle and mining height of the working face F5001 are constantly changing, and the backfilling technology is relatively complex. The inclined mining is not conducive to the backfilling of working face. To improve the backfilling quality in the inclined mining, the

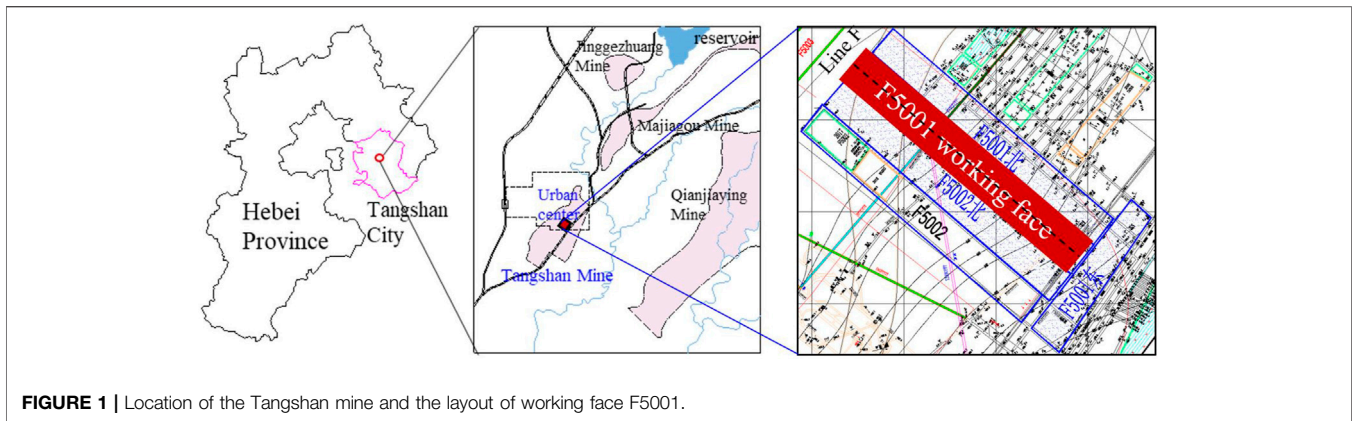


FIGURE 1 | Location of the Tangshan mine and the layout of working face F5001.

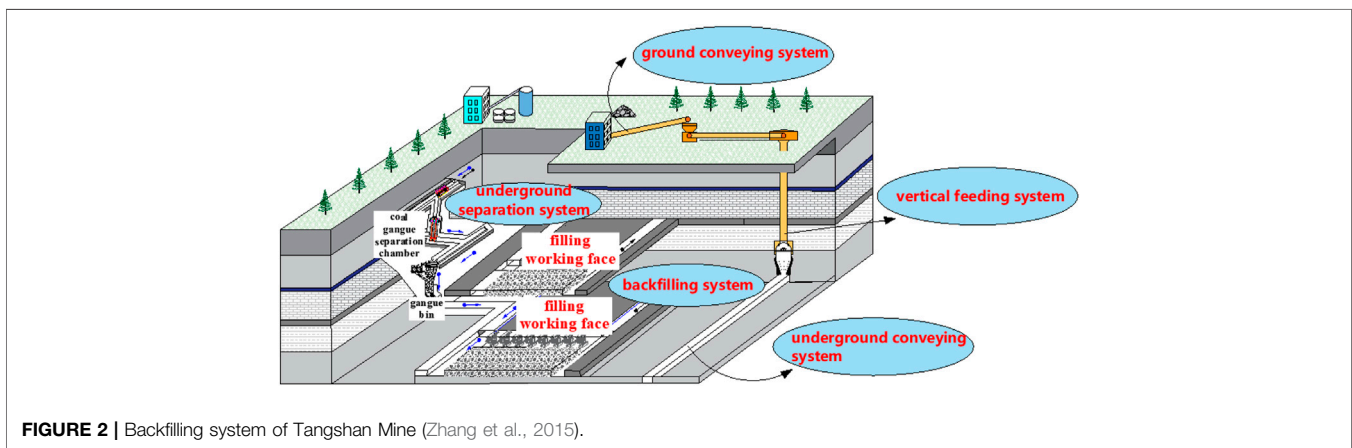


FIGURE 2 | Backfilling system of Tangshan Mine (Zhang et al., 2015).

following points should be ensured: 1) the compaction force should be appropriately increased (Ye et al., 2010; Yanli et al., 2011; Zhou et al., 2016), and the compaction force should no less than 2.5 MPa; 2) a small amount of backfilling materials should be discharged at sections, and the number of compaction and single-hole discharge should be increased to ensure the backfilling body can fully connect with the roof (Chen et al., 2002; Komine, 2004; Latha and Krishna, 2008). It can be seen that compaction force is the key point of backfilling technology research.

VERIFICATION OF LABORATORY GANGUE COMPACTION TEST RESULTS

Materials and Test Systems

The gangue samples were taken from washing gangue and excavated gangue in the mining area F of Tangshan mine. The main lithology of gangue samples was sandy mudstone. Before the test, the gangue samples were crushed. The crusher was used to break the gangue to obtain gangue samples with a particle size of less than 30 mm (Cihangir et al., 2012; Grgic et al., 2013; Han et al., 2016), and then the grading screen was used to grade the original gangue. The grading of particle size was 0–5 mm, 5–10 mm, 10–15 mm, 15–20 mm, 20–25 mm and 25–30 mm, respectively.

The uniaxial loading test system of gangue backfilling material (Komine, 2010; Brzesowsky et al., 2014; Miao et al., 2016) was developed, which was mainly composed of the axial loading system, steel cylinder, data monitoring and acquisition system. The compaction test was carried out on the electro-hydraulic servo universal testing system, which includes the WAW-1000D microcomputer controlled electro-hydraulic servo universal testing machine and the self-made compaction steel cylinder. The maximum loading force provided by the testing machine was 1000 KN. The self-made compaction steel cylinder was composed of the steel cylinder, base, dowel bar and loading plate. The inner diameter of the steel cylinder was 250 mm, the outer diameter was 274 mm, the height was 305 mm, and the wall thickness was 12 mm. The steel cylinder and the base were connected by the flange. The radius of the loading plate was 124 mm and the height was 40 mm, which can realize the uniform stress of the sample in the loading process. Figure 3 shows gangue samples and the test system.

Test Principle and Scheme

Test Principle

The axial loading force was used to simulate the compaction force in the field (Helwany et al., 1999; Ahmadabadi and Ghanbari, 2009; Yan et al., 2021). After the initial loading stress was applied,

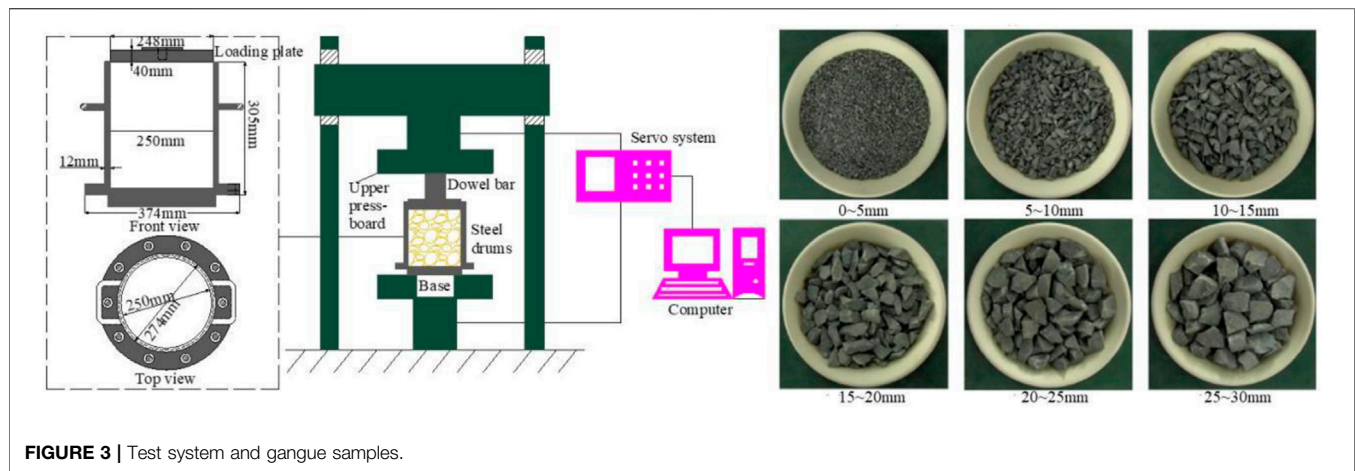


FIGURE 3 | Test system and gangue samples.

a final loading force of 735 kN (15MPa) was applied, and the final compaction deformation of gangue backfilling materials was recorded. The test principle is as follows:

The strain of the sample is:

$$\varepsilon = \frac{\Delta h}{h} \quad (1)$$

where ε is the strain, Δh is the compression deformation and h is the initial loading height before compaction.

The relationship between stress and bulk density is as follows

$$\rho(\sigma) = \frac{\rho_0}{1 - \varepsilon(\sigma)} \quad (2)$$

where ρ_0 is the initial density of gangue, 2.4 t/m^3 .

There is no fixed parameter to express the stress-strain relationship of gangue, and the deformation modulus of gangue is defined as $E = \sigma/\varepsilon$, and the elastic foundation coefficient of the backfilling body is $k_g = E/h$. During the compaction, the relationship between stress and elastic foundation coefficient is as follows:

$$k_g = \frac{\sigma}{\varepsilon h} \quad (3)$$

Test Scheme

According to the grading of gangue, six graded particle sizes are 0–5, 5–10, 10–15, 15–20, 20–25, and 25–30 mm, which are named as g1, g2, g3, g4, g5 and g6, respectively. The gangue with different particle size was proportioned evenly, i.e. g1: g2: g3: g4: g5: g6 = 1:1: 1:1:1:1:1:1. The compaction deformation characteristics of six kinds of particle size gangue and uniform graded gangue were tested, and then the compaction and deformation characteristics of seven groups of samples were studied.

Test Results

Stress-Strain Relationship

The stress-strain curve of gangue during compaction is obtained, as shown in Figure 4. The comparison of gangue strain in each stage is shown in Table 1.

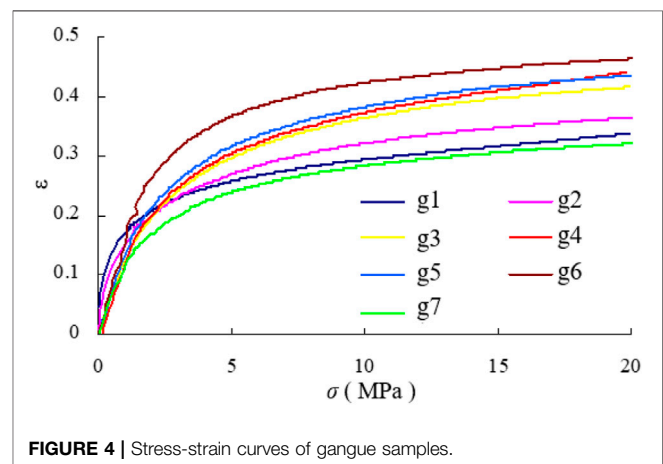


FIGURE 4 | Stress-strain curves of gangue samples.

As shown in Figure 4 and Table 1, the stress-strain curve of the gangue sample generally shows a logarithmic distribution trend. In the initial compaction stage (0–2.5 MPa), the strain increases by 16.6–25.8%, and the gangue sample has a rapid deformation rate. With the gradual increase of axial loading, the gangue sample is compacted gradually, and the strain growth decreases gradually.

Relationship Between Stress and Bulk Density

The stress bulk density curve of gangue samples in the compaction process is obtained, as shown in Figure 5. The variation of gangue bulk density in different stages is shown in Table 2.

As illustrated in Figure 5 and Table 2, with the increase of the compaction force, the bulk density of the backfilling material increases. The bulk density of the backfilling material is $22.2\text{--}17.6 \text{ kN m}^{-3}$ under the compaction force of 0–2.5MPa. With the increase of compaction force, the deformation of gangue samples increases gradually. The bulk density increases slowly in the later compaction stage, which is represented by the gentle curve in the later compaction stage.

TABLE 1 | Strain variable of gangue samples at different stages.

| | Uniform proportioning (%) | 0–50 mm (%) | 5–50 mm (%) | 10–50 mm (%) | 15–50 mm (%) | 20–50 mm (%) | 25–50 mm (%) |
|-----------|---------------------------|-------------|-------------|--------------|--------------|--------------|--------------|
| 2.5 MPa | 16.6 | 19.7 | 20.4 | 20.8 | 21.3 | 23.0 | 25.8 |
| 15 MPa | 30.6 | 31.0 | 34.7 | 39.0 | 40.3 | 41.6 | 42.4 |
| 2.5–15MPa | 14.0 | 11.3 | 14.3 | 18.2 | 19.0 | 18.6 | 16.6 |

TABLE 2 | Variation of bulk density of gangue samples in different stages.

| | Uniform proportioning | 0–50 mm | 5–50 mm | 10–50 mm | 15–50 mm | 20–50 mm | 25–50 mm |
|---|-----------------------|---------|---------|----------|----------|----------|----------|
| Original bulk density/(kN m ⁻³) | 18.5 | 16.2 | 15.3 | 14.7 | 13.7 | 13.4 | 13.0 |
| Bulk density at the 2.5MPa/(kN m ⁻³) | 22.2 | 20.3 | 19.1 | 17.9 | 16.9 | 16.7 | 17.6 |
| Mass ratio of mining and backfilling after compaction | 1.49 | 1.36 | 1.28 | 1.20 | 1.14 | 1.12 | 1.18 |

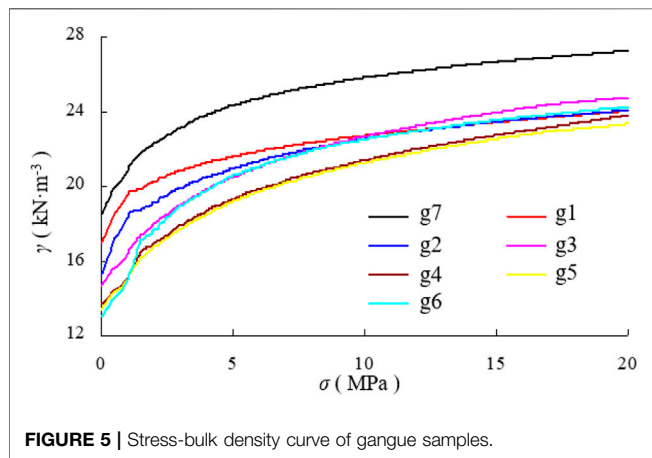


FIGURE 5 | Stress-bulk density curve of gangue samples.

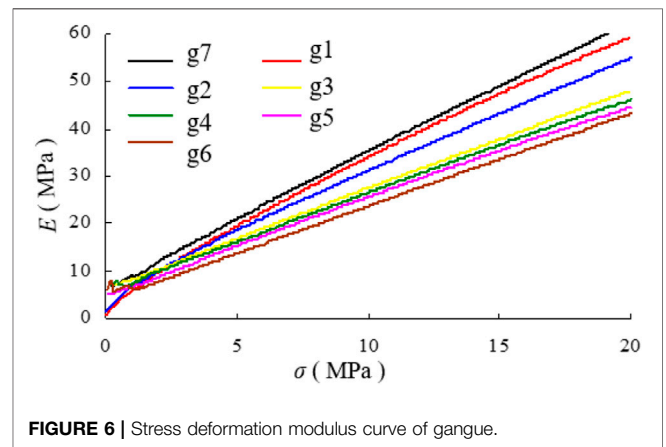


FIGURE 6 | Stress deformation modulus curve of gangue.

Relationship Between Stress and Deformation Modulus

The stress deformation modulus curve of gangue during compaction is shown in **Figure 6**, and the variation of deformation modulus of gangue at different stages is shown in **Table 3**.

As shown in **Figure 6** and **Table 3**, with the increase of pressure σ , the deformation modulus E of gangue samples with different particle sizes increases, and the changing range of E is 0–60 MPa. Compared with the elastic modulus of intact gangue, the order of magnitude of the granular material composed of broken gangue particles is quite different. When the compressive strength reaches 15 MPa, the deformation modulus is about 28–50 MPa.

FIELD TEST ON LONG-TERM COMPACTION CHARACTERISTICS OF GANGUE SAMPLES

According to test results in the laboratory, 2.5 MPa is the optimal compaction force. In the actual backfilling operation of working face F5001, the compaction force of 2.5 MPa was adopted, and the backfilling materials were discharged and backfilled at sections.

Principle and Scheme of Compaction Characteristics in the On-Site Measurement

The mass ratio of mining and backfilling refers to the mass ratio of coal and gangue. Through monitoring the mass ratio of mining and backfilling, the compaction characteristics of gangue are further converted in the Tangshan mine. According to the formula of the mass ratio of mining and backfilling, it is obtained as follows:

$$\frac{1}{c} = \frac{m_c}{m_g} = \frac{v_c \cdot \rho_c}{v_g \cdot \rho_g} = \frac{h_0}{h_0 - \Delta h} \frac{\rho_c}{\rho_g} = \frac{1}{1 - \varepsilon} \frac{\rho_c}{\rho_g} \quad (4)$$

$$E = \frac{\sigma_0}{\varepsilon} \quad (5)$$

TABLE 3 | Variation of deformation modulus of gangue in different stages.

| No | Particle size grade | E- σ equation |
|----|-----------------------|-----------------------------|
| 1 | Uniform proportioning | $E = 2.7958\sigma + 6.7557$ |
| 2 | 0–50 mm | $E = 2.8311\sigma + 4.7453$ |
| 3 | 5–50 mm | $E = 2.5159\sigma + 5.4693$ |
| 4 | 10–50 mm | $E = 2.1014\sigma + 6.3100$ |
| 5 | 15–50 mm | $E = 2.0366\sigma + 5.9730$ |
| 6 | 20–50 mm | $E = 2.0098\sigma + 5.1370$ |
| 7 | 25–50 mm | $E = 1.9578\sigma + 4.0882$ |



FIGURE 7 | Distribution of mass ratio of mining and backfilling in coal mining.

TABLE 4 | Mass ratio of mining and backfilling and deformation modulus data in coal mining.

| Date | 2016/10 | 2016/11 | 2016/12 | 2017/1 | 2017/2 | 2017/3 | 2017/4 | 2017/5 | 2017/6 | 2017/7 | 2017/8 | 2017/9 |
|--------------------------------------|---------|---------|---------|--------|--------|--------|--------|--------|--------|--------|--------|--------|
| Cumulative advancing distance | 24 | 96 | 103 | 138 | 138 | 138 | 213 | 313 | 403 | 495 | 585 | 640 |
| Mass ratio of mining and backfilling | 1.86 | 1.21 | 1.2 | 1.31 | 0 | 0 | 1.29 | 1.28 | 1.30 | 1.30 | 1.30 | 1.31 |
| Deformation modulus | 21.88 | 29.03 | 29.26 | 27.10 | 0 | 0 | 27.49 | 27.62 | 27.26 | 27.26 | 27.21 | 27.10 |

where c is the mass ratio of mining to backfilling; ϵ is the test strain; ρ_c is the density of coal, $\text{kg}\cdot\text{m}^{-3}$; ρ_g is the density of gangue, $\text{kg}\cdot\text{m}^{-3}$; σ_0 is the vertical stress and E is the deformation modulus.

Due to the change in the inclination angle and mining height during the actual mining process, the angles of -5° , 0° , 10° , 15° , and 20° were used, and the mining heights of 2.2, 2.4, 2.6, 2.8, and 3.0 m were selected. In this way, the mass ratio of mining and backfilling under different advancing distances, inclination angles and mining heights were explored.

On-Site Measurement Results of Compaction Characteristics

On-Site Measurement of Compaction Characteristics of Gangue During Advancing

With the advance in the working face from October 2016 to September 2017, the distribution of mass ratios of the mining and backfilling is shown in Figure 7. The deformation modulus data converted from the mass ratio of mining and backfilling is shown in Table 4. During this period, 211,439 t gangue was filled and 164,127 t coal was mined.

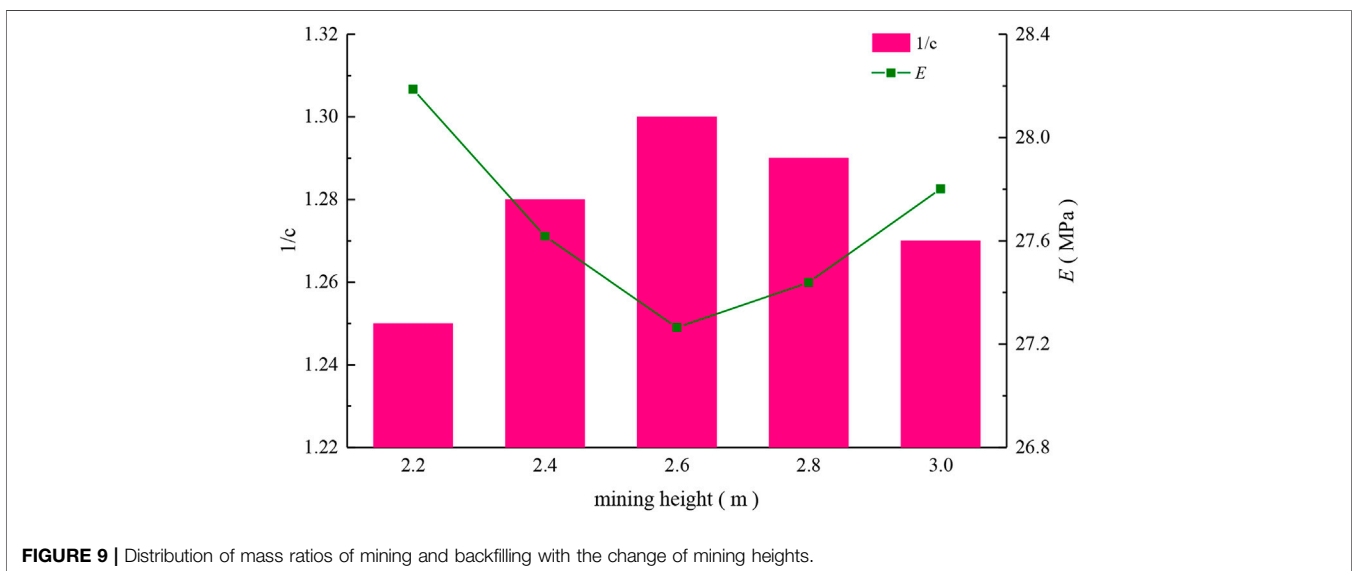
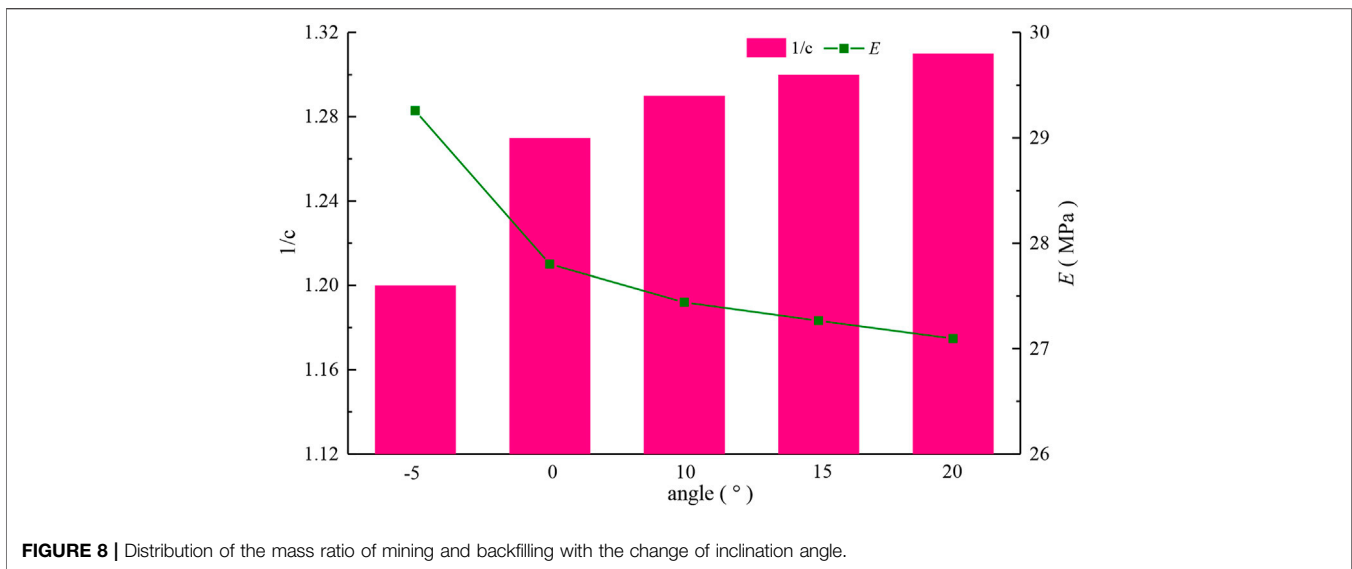
As shown in Figure 7 and Table 4, during the initial mining in the working face, the roof condition of the goaf is good and more gangue can be filled in the goaf. With the continuous advancement of the working face, the mass ratio of mining and backfilling is stable at about 1.30.

The deformation modulus of the final gangue backfilling body remains at about 27 MPa under the compaction state, which is slightly smaller than the data measured in the laboratory.

Experimental Study on Compaction Characteristics of Gangue Under Different Inclination Angles and Mining Heights

With the change of inclination angles, the distribution of the mass ratio of mining and backfilling is obtained, as shown in Figure 8. It can be seen that with the increase of inclination angle, the mining in the working face gradually changes from downward mining to upward mining, and the mass ratio of mining and backfilling gradually increases, which is conducive to backfilling in goaf. However, the deformation modulus of the backfilling body decreases gradually, and the deformation resistance of the backfilling body weakens. Thus, the larger inclination angle in the upward mining is not beneficial to the backfilling.

With the change of mining heights, the distribution of mass ratios of mining and backfilling is shown in Figure 9, and the deformation modulus data converted from these mass ratios are obtained. As shown in Figure 9, with the increase of mining height, the mass ratio of mining and backfilling first increases and then decreases, indicating that the mining height of 2.6 m is more conducive to backfilling. The deformation modulus of gangue backfilling body is the smallest at the mining height of 2.6 m. It can be concluded that the smaller



the deformation resistance of gangue, the more gangue can be filled.

SURFACE SUBSIDENCE MONITORING AND CONTROL EFFECT

Surface Subsidence Monitoring System

The surface subsidence monitoring system includes Beidou satellite navigation system, Beidou satellite reference station and CORS monitoring system (Rollins and Sparks, 2002; Liu et al., 2009; Hla et al., 2021). This system can automatically and accurately monitor the surface subsidence above the working face all day. CORS monitoring system includes data center, reference station, data communication subsystem and user application

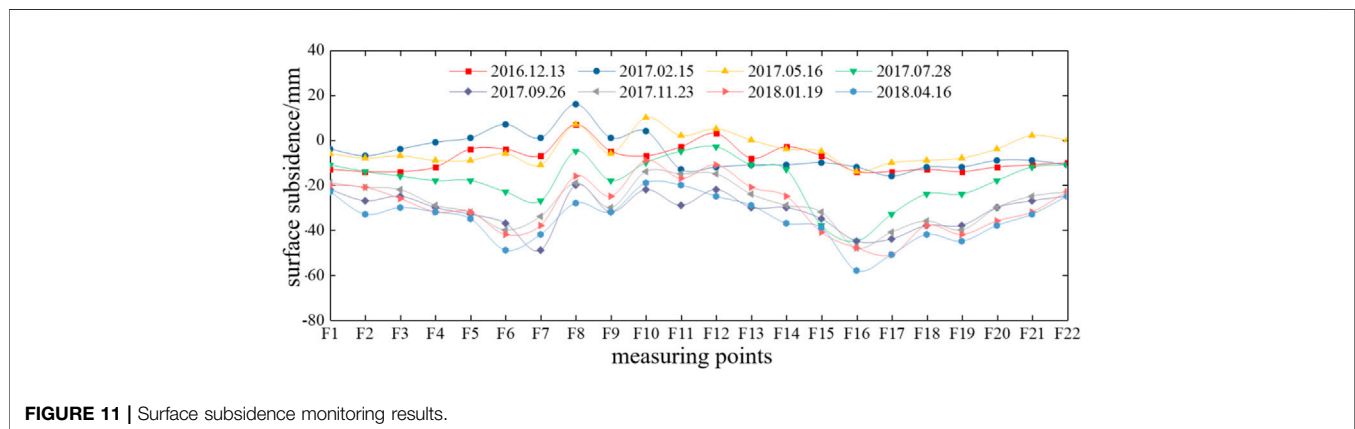
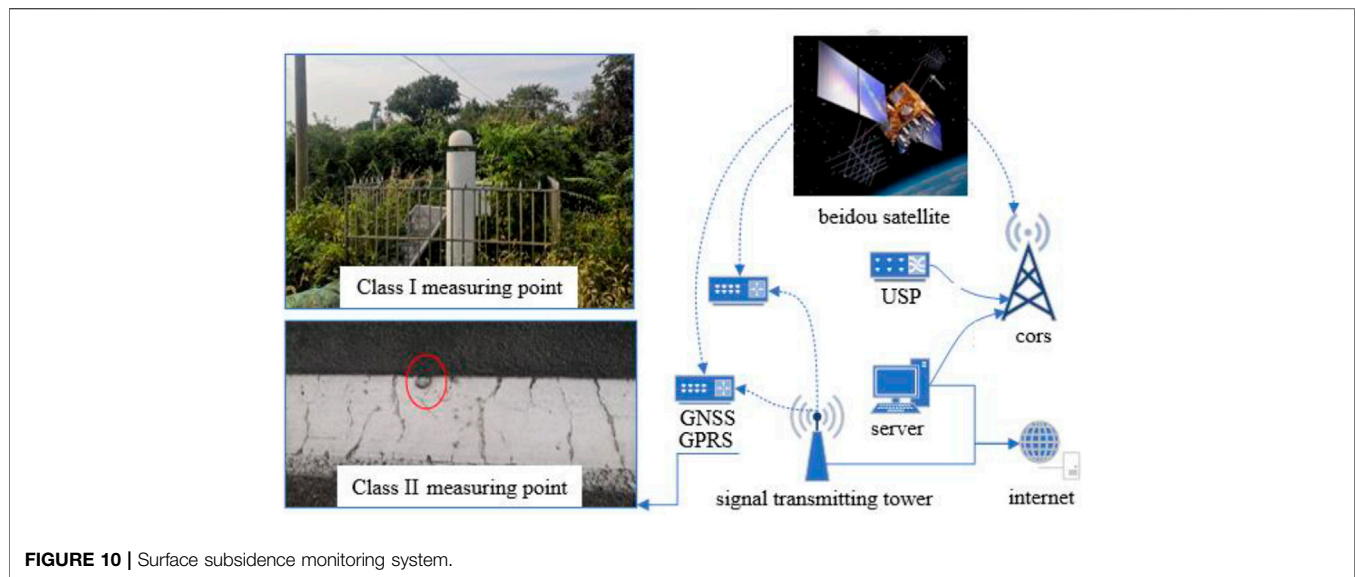
subsystem, which greatly improves the accuracy of surface subsidence measurement. The monitoring system is shown in Figure 10.

Surface Subsidence Monitoring Scheme

The ground position of working face F5001 crossed Jianshe South Road and Daxue Road, and was adjacent to the mining area railway in the east. A surface observation line F was set on the surface of working face F5001, and a total of 22 measuring points were set along the line to observe the influence of mining on the surface subsidence of working face F5001.

Surface Subsidence Monitoring Results

The surface subsidence test results of the working face F5001 are shown in Figure 11.



From December 2016 to May 2017, the surface subsidence increased slowly, and the subsidence value was less than 20 mm. From May 2017 to July 2017, the surface subsidence increased significantly, but the total subsidence was still in a small range, and the maximum subsidence was 45 mm at the measuring point of F16. In November 2017, the working face was fully mined; in April 2018, the maximum subsidence increased to 61 mm at the measuring point of F12, which was a small increase in 3 months. Therefore, it can be considered that working face F5001 was fully affected by the mining activities in January 2018.

According to the surface subsidence value in the measuring line F of the working face F5001 in April 2018, the surface tilt deformation, curvature deformation, horizontal displacement and horizontal deformation at different measuring points were calculated. The maximum surface tilt deformation value was 1.65 mm/m, which appeared at the measuring point of F12. The maximum curvature deformation value was 0.094 mm/m², which occurred at the measuring point of F17; the maximum deformation value in the horizontal displacement was 16.1 mm, and the maximum horizontal deformation value was 1.25 mm/m, which also occurred at the measuring point of F17.

The maximum surface subsidence value was 61 mm, and the value met the fortification standard of “Regulations for coal pillar setting of buildings, water bodies, railways and main shafts and coal pressed mining” (Ma et al., 2019; Ma et al., 2021a) in 2017. With the advance of the working face, the surface of the ground sank slowly. When the advancing speed of the working face increased, the surface subsidence rate increased, and the curve in **Figure 11** was steeper. In other words, the greater the advancing speed, the greater the sinking speed. After the mining, the surface subsidence rate decreased obviously, even tended to be constant. It indicated that the strata moved slowly and tended to be stable after backfilling mining, which is helpful to the protection of surface buildings.

CONCLUSION

In this study, the uniaxial loading test system of gangue backfilling material was developed, and the basic compaction characteristics of gangue were obtained, such as stress-strain relationship, relationship between stress and bulk density, and relationship

between stress and deformation modulus. The test results show that the initial loading stress of 2.5 MPa can ensure the large deformation characteristics of gangue.

Based on the on-site measurement of the compaction characteristics of the gangue backfilling body in the Tangshan mine, the deformation modulus of the working face with different inclination angles and mining heights was studied. The results show that the field measurement data are consistent with the laboratory test data, and the deformation modulus of the gangue after compaction is close to 27 MPa.

After the backfilling in the working face F5001, the Beidou satellite CORS monitoring system has been used to monitor the surface subsidence for 2 years. The monitoring results show that the surface deformation is effectively controlled, and the maximum surface subsidence is limited to 61 mm.

DATA AVAILABILITY STATEMENT

The original contributions presented in the study are included in the article/Supplementary Material, further inquiries can be directed to the corresponding authors.

REFERENCES

- Ahmadabadi, M., and Ghanbari, A. (2009). New Procedure for Active Earth Pressure Calculation in Retaining walls with Reinforced Cohesive-Frictional Backfill. *Geotextiles and Geomembranes* 27 (6), 456–463. doi:10.1016/j.geotextmem.2009.06.004
- Benzaazoua, M., Ouellet, J., Servant, S., Newman, P., and Verburg, R. (1999). Cementitious Backfill with High Sulfur Content Physical, Chemical, and Mineralogical Characterization. *Cement Concrete Res.* 29 (5), 719–725. doi:10.1016/S0008-8846(99)00023-X
- Brzesowsky, R. H., Hangx, S. J. T., Brantut, N., and Spiers, C. J. (2014). Compaction Creep of Sands Due to Time-Dependent Grain Failure: Effects of Chemical Environment, Applied Stress, and Grain Size. *J. Geophys. Res. Solid Earth* 119 (10), 7521–7541. doi:10.1002/2014JB011277
- Cao, L.-M., Sun, S.-J., Zhang, Y.-Z., Guo, H., and Zhang, Z. (2018). The Research on Characteristics of Hydraulic Support Advancing Control System in Coal Mining Face. *Wireless Pers Commun.* 102, 2667–2680. doi:10.1007/s11277-018-5294-4
- Chen, S. L., Feng, X. T., and Li, S. J. (2002). Effects of Chemical Erosion on Mechanical Behaviors of Xiaolangdi Sandstone. *Rock Soil Mech.* 23 (3), 284–283. doi:10.1007/s11769-002-0073-1
- Chong, Z., Yao, Q., Li, X., and Shivakumar, K. (2020). Acoustic Emission Investigation on Scale Effect and Anisotropy of Jointed Rock Mass by the Discrete Element Method. *Arab J. Geosci.* 13 (9), 1–14. doi:10.1007/s12517-020-05303-z
- Cihangir, F., Ercikdi, B., Kesimal, A., Turan, A., and Deveci, H. (2012). Utilisation of Alkali-Activated Blast Furnace Slag in Paste Backfill of High-Sulphide Mill Tailings: Effect of Binder Type and Dosage. *Minerals Eng.* 30, 33–43. doi:10.1016/j.mineng.2012.01.009
- Dai, G., Sheng, Y., Li, S., and Zhang, Y. (2018). Experimental Study on Mechanical Properties of Anti-Seepage Slurry in Landfill. *Mod. Phys. Lett. B* 32, 1840065. doi:10.1142/S0217984918400651
- Ercikdi, B., Cihangir, F., Kesimal, A., Deveci, H., and Alp, İ. (2009). Utilization of Industrial Waste Products as Pozzolanic Material in Cemented Paste Backfill of High Sulphide Mill Tailings. *J. Hazard. Mater.* 168 (2-3), 848–856. doi:10.1016/j.jhazmat.2009.02.100
- Fall, M., Benzaazoua, M., and Saa, E. G. (2008). Mix Proportioning of Underground Cemented Tailings Backfill. *Tunnelling Underground Space Technol.* 23 (1), 80–90. doi:10.1016/j.tust.2006.08.005
- Fall, M., Célestin, J. C., Pokharel, M., and Touré, M. (2010). A Contribution to Understanding the Effects of Curing Temperature on the Mechanical

AUTHOR CONTRIBUTIONS

JW: Conceptualization, Model investigation, Data curation, Writing—original draft. QZ: Model investigation, Laboratorial investigation, Data curation. WY: Funding acquisition, Writing—review and editing. SQ: Data curation. DG: Laboratorial investigation, Data curation. DM: Conceptualization, Funding acquisition Data curation.

FUNDING

This work is funded by Independent Research Project of the National Natural Science Foundation of China (52174134, 51904110, 51804339, 41977238 and 52122404) and the Fundamental Research Funds for the Central Universities (2021GJZPY12).

ACKNOWLEDGMENTS

Thanks to the staff of Tangshan mine, they worked hard to monitor and got precious measured data.

- Properties of Mine Cemented Tailings Backfill. *Eng. Geology.* 114 (3-4), 397–413. doi:10.1016/j.enggeo.2010.05.016
- Grgic, D., Giraud, A., and Auvray, C. (2013). Impact of Chemical Weathering on Micro/Macro-Mechanical Properties of Oolitic Iron Ore. *Int. J. Rock Mech. Mining Sci.* 64, 236–245. doi:10.1016/j.ijrmmms.2013.09.005
- Han, T., Shi, J., and Cao, X. (2016). Fracturing and Damage to Sandstone Under Coupling Effects of Chemical Corrosion and Freeze-Thaw Cycles. *Rock Mech. Rock Eng.* 49 (11), 4245–4255. doi:10.1007/s00603-016-1028-7
- Hawkes, I., and Fellers, G. E. (1969). Theory of the Determination of the Greatest Principal Stress in a Biaxial Stress Field Using Photoelastic Hollow cylinder Inclusions. *Int. J. Rock Mech. Mining Sci. Geomechanics Abstr.* 6 (2), 143–158. doi:10.1016/0148-9062(69)90032-1
- Helwany, S. M. B., Reardon, G., and Wu, J. T. H. (1999). Effects of Backfill on the Performance of Grs Retaining walls. *Geotextiles and Geomembranes* 17 (1), 1–16. doi:10.1016/S0266-1144(98)00021-1
- Komine, H. (2004). Simplified Evaluation on Hydraulic Conductivities of Sand-Bentonite Mixture Backfill. *Appl. Clay Sci.* 26 (1/4), 13–19. doi:10.1016/j.clay.2003.09.006
- Komine, H. (2010). Predicting Hydraulic Conductivity of Sand-Bentonite Mixture Backfill before and after Swelling Deformation for Underground Disposal of Radioactive Wastes. *Eng. Geology.* 114 (3-4), 123–134. doi:10.1016/j.enggeo.2010.04.009
- Latha, G. M., and Krishna, A. M. (2008). Seismic Response of Reinforced Soil Retaining wall Models: Influence of Backfill Relative Density. *Geotextiles and Geomembranes* 26 (4), 335–349. doi:10.1016/j.geotextmem.2007.11.001
- Li, K., and Sheng, P. (1995). Plane Stress Model for Fracture of Ceramics during Laser Cutting. *Int. J. Machine Tools Manufacture* 35 (11), 1493–1506. doi:10.1016/0890-6955(94)00127-6
- Li, H., Guo, G., and Zheng, N. (2018). Influence of Coal Types on Overlying Strata Movement and Deformation in Underground Coal Gasification without Shaft and Prediction Method of Surface Subsidence. *Process Saf. Environ. Prot.* 120, 302–312. doi:10.1016/j.psep.2018.09.023
- Liu, H., Wang, X., and Song, E. (2009). Long-Term Behavior of Grs Retaining walls with Marginal Backfill Soils. *Geotextiles and Geomembranes* 27 (4), 295–307. doi:10.1016/j.geotextmem.2009.01.002
- Liu, H., Zhang, J., Li, B., Zhou, N., Li, D., Zhang, L., et al. (2021). Long Term Leaching Behavior of Arsenic from Cemented Paste Backfill Made of Construction and Demolition Waste: Experimental and Numerical Simulation Studies. *J. Hazard. Mater.* 416, 125813. doi:10.1016/j.jhazmat.2021.125813

- Li, M., Zhang, J.-x., Huang, P., and Gao, R. (2016). Mass Ratio Design Based on Compaction Properties of Backfill Materials. *J. Cent. South. Univ.* 23, 2669–2675. doi:10.1007/s11771-016-3328-1
- Livaoglu, R., Cakir, T., Dogangun, A., and Aytekin, M. (2011). Effects of Backfill on Seismic Behavior of Rectangular Tanks. *Ocean Eng.* 38 (10), 1161–1173. doi:10.1016/j.oceaneng.2011.05.017
- Louréno, P. B., De Borst, R., and Rots, J. G. (1997). A Plane Stress Softening Plasticity Model for Orthotropic Materials. *Int. J. Numer. Methods Eng.* 40 (21), 4033–4057. doi:10.1002/(SICI)1097-0207(19971115)40:21<4033::AID-NME248>3
- Ma, D., Wang, J., Cai, X., Ma, X., Zhang, J., Zhou, Z., et al. (2019). Effects of Height/Diameter Ratio on Failure and Damage Properties of Granite under Coupled Bending and Splitting Deformation. *Eng. Fracture Mech.* 220, 106640. doi:10.1016/j.engfractmech.2019.106640
- Ma, D., Kong, S., Li, Z., Zhang, Q., Wang, Z., and Zhou, Z. (2021a). Effect of Wetting-Drying Cycle on Hydraulic and Mechanical Properties of Cemented Paste Backfill of the Recycled Solid Wastes. *Chemosphere* 282, 131163. doi:10.1016/j.chemosphere.2021.131163
- Ma, D., Zhang, J., Duan, H., Huang, Y., Li, M., Sun, Q., et al. (2021b). Reutilization of Gangue Wastes in Underground Backfilling Mining: Overburden Aquifer Protection. *Chemosphere* 264 (Pt 1), 128400. doi:10.1016/j.chemosphere.2020.128400
- Malusis, M. A., Barben, E. J., and Evans, J. C. (2009). Hydraulic Conductivity and Compressibility of Soil-Bentonite Backfill Amended with Activated Carbon. *J. Geotech. Geoenviron. Eng.* 135 (5), 664–672. doi:10.1061/(ASCE)GT.1943-5606.00000041
- Miao, S., Cai, M., Guo, Q., Wang, P., Liang, M., et al. (2016). Damage Effects and Mechanisms in Granite Treated with Acidic Chemical Solutions. *Int. J. Rock Mech. Mining Sci.* 88, 77–86. doi:10.1016/j.ijrmms.2016.07.002
- Mitchell, R. J., Olsen, R. S., and Smith, J. D. (2011). Model Studies on Cemented Tailings Used in Mine Backfill. *Can. Geotech. J.* 19 (1), 14–28. doi:10.1139/t82-002
- Niu, D. X., Wang, P., Wang, Q., Hua, F. Y., Wang, F., and Cai, Z. H. (2014). Analysis of the Power Plant Security Management Capability Based on the Ism and Ahp. *Adv. Mater. Res.* 960-961, 1477–1482. doi:10.4028/www.scientific.net/AMR960-961.1477
- Rollins, K. M., and Sparks, A. (2002). Lateral Resistance of Full-Scale Pile Cap with Gravel Backfill. *J. Geotech. Geoenviron. Eng.* 128 (9), 711–723. doi:10.1061/(asce)1090-0241(2002)128:9(711)
- Shukla, S. K., Gupta, S. K., and Sivakugan, N. (2009). Active Earth Pressure on Retaining Wall for C- ϕ Soil Backfill under Seismic Loading Condition. *J. Geotech. Geoenviron. Eng.* 135 (5), 690–696. doi:10.1061/(ASCE)GT.1943-5606.00000003
- Wei, H., Wen, Z., Ba, L., and Gao, Q. (2021). Study on Strength Test and Hydration Mechanism of Phosphogypsum Based Cemented Backfill. *IOP Conf. Ser. Earth Environ. Sci.* 768 (1), 012100. doi:10.1088/1755-1315/768/1/012100
- Wijewickreme, D., and Vaid, Y. P. (1993). Behaviour of Loose Sand under Simultaneous Increase in Stress Ratio and Principal Stress Rotation. *Can. Geotech. J.* 30 (6), 953–964. doi:10.1139/t93-093
- Xie, H. P., Zhou, H. W., Xue, D. J., Wang, H. W., Zhang, R., and Gao, F. (2012). Research and Consideration on Deep Coal Mining and Critical Mining Depth. *J. China Coal Soc.* 37 (37), 535–542. doi:10.1007/s11783-011-0280-z
- Xie, H., Feng, G., Yang, J. U., and University, S. (2015a). Research and Development of Rock Mechanics in Deep Ground Engineering. *Chin. J. Rock Mech. Eng.* 11, 2161–2178. doi:10.13722/j.cnki.jrme.2015.1369
- Xie, H. P., Gao, F., Ju, Y., Gao, M. Z., Zhang, R., and Gao, Y. N. (2015b). Quantitative Definition and Investigation of Deep Mining. *J. China Coal Soc.* 40 (1), 1–10. doi:10.13225/j.cnki.jccs.2014.1690
- Yan, H., Zhang, J., Li, B., and Zhu, C. (2021). Crack Propagation Patterns and Factors Controlling Complex Crack Network Formation in Coal Bodies during Tri-axial Supercritical Carbon Dioxide Fracturing. *Fuel* 286, 119381. doi:10.1016/j.fuel.2020.119381
- Yanli, H., Jixiong, Z., Baifu, A., and Qiang, Z. (2011). Overlying Strata Movement Law in Fully Mechanized Coal Mining and Backfilling Longwall Face by Similar Physical Simulation. *J. Min. Sci.* 47 (5), 618–627. doi:10.1134/S1062739147050108
- Ye, W.-M., Chen, Y.-G., Chen, B., Wang, Q., and Wang, J. (2010). Advances on the Knowledge of the Buffer/backfill Properties of Heavily-Compacted Gmz Bentonite. *Eng. Geology.* 116 (1-2), 12–20. doi:10.1016/j.enggeo.2010.06.002
- Yuan, Y., and Sun, H. (2012). A Novel Silica Alumina-Based Backfill Material Composed of Coal Refuse and Fly Ash. *J. Hazard. Mater.* 213-214, 71–82. doi:10.1016/j.jhazmat.2012.01.059
- Zhang, Q.-L., and Wang, X.-M. (2007). Performance of Cemented Coal Gangue Backfill. *J. Cent. South. Univ. Technol.* 14 (2), 216–219. doi:10.1007/s11771-007-0043-y
- Zhang, J., Zhang, Q., Sun, Q., Gao, R., Germain, D., and Abro, S. (2015). Surface Subsidence Control Theory and Application to Backfill Coal Mining Technology. *Environ. Earth Sci.* 74 (2), 1439–1448. doi:10.1007/s12665-015-4133-0
- Zhou, N., Han, X., Zhang, J., and Li, M. (2016). Compressive Deformation and Energy Dissipation of Crushed Coal Gangue. *Powder Technol.* 297, 220–228. doi:10.1016/j.powtec.2016.04.026
- Zhu, C., Yuan, Y., Yuan, C. f., Liu, F. Q., Chen, Z. S., and Wang, S. Z. (2020). Study on the Structural Forms of the Key Strata in the Overburden of a Stope during Periodic Weighting and the Reasonable Working Resistance of the Support. *Energy Sci Eng* 8, 2599–2620. doi:10.1002/ese3.688

Conflict of Interest: The authors declare that the research was conducted in the absence of any commercial or financial relationships that could be construed as a potential conflict of interest.

Publisher's Note: All claims expressed in this article are solely those of the authors and do not necessarily represent those of their affiliated organizations, or those of the publisher, the editors and the reviewers. Any product that may be evaluated in this article, or claim that may be made by its manufacturer, is not guaranteed or endorsed by the publisher.

Copyright © 2021 Wang, Zhang, Yin, Qi, Gao and Ma. This is an open-access article distributed under the terms of the Creative Commons Attribution License (CC BY). The use, distribution or reproduction in other forums is permitted, provided the original author(s) and the copyright owner(s) are credited and that the original publication in this journal is cited, in accordance with accepted academic practice. No use, distribution or reproduction is permitted which does not comply with these terms.